Optics Letters

Multiple beam coherent combination via an optical ring resonator

Nina Bode,[1,†] Zachary Holmes,[2,3,†] Sebastian Ng,[2,3] Benjamin von Behren,[1] David Ottaway,[2,3] and Benno Willke[1,*]

[1]Max Planck Institute for Gravitational Physics (Albert Einstein Institute) and Institut für Gravitationsphysik, Leibniz Universität Hannover, Hannover, Germany
[2]Department of Physics and The Institute for Photonics and Advanced Sensing (IPAS), The University of Adelaide, SA 5005, Australia
[3]OzGrav, The Australian Research Council Centre of Excellence for Gravitational Wave Discovery, Australia
[†]These authors contributed equally to this Letter.
*benno.willke@aei.mpg.de

Received 14 July 2023; revised 11 August 2023; accepted 14 August 2023; posted 15 August 2023; published 1 September 2023

Future gravitational wave detectors (GWDs) require low noise, single frequency, continuous wave lasers with excellent beam quality and powers in excess of 500 W. Low noise laser amplifiers with high spatial purity have been demonstrated up to 300 W. For higher powers, coherent beam combination can overcome scaling limitations. In this Letter we introduce a new, to the best of our knowledge, combination scheme that uses a bow-tie resonator to combine three laser beams with simultaneous spatial filtering performance.

https://doi.org/10.1364/OL.500684

Next-generation gravitational wave detectors (GWDs) will require megawatts of power in their arm cavities to achieve their scientific goals [1,2]. To build up 5 MW of arm cavity power, it is anticipated that up to 700 W of laser output is required of an ultra-stable, single-frequency, diffraction-limited source [1,2].

A single laser source has not been demonstrated that can deliver such high powers while simultaneously satisfying the stringent beam quality and spectral requirements. Solid-state bulk crystal lasers and amplifiers have demonstrated 220 W of laser power at 1064 nm with suitable performance [3–6]. The power of bulk laser systems is limited by thermally induced optical deformation and potential failure due to thermal gradients generated in high-power operation. Fiber-based lasers offer far greater thermal stability with high surface area to volume ratios but they encounter performance-limiting optical nonlinearities, namely stimulated Brillouin scattering [7]. The power limitations of these single sources can be circumvented with the coherent beam combination (CBC) of multiple sources. CBC schemes for GWDs have been under investigation for several decades [8–11], including a recent demonstration of 370 W of linear polarized light in the TEM00 mode at 1064 nm [12]. These experiments used a beam splitter as a combining optic. Multiple beams can be combined with cascaded beam splitters, introducing greater complexity with an additional beam splitter required for every added beam and the need for a nested phase control scheme. Alternatively, a resonator can combine multiple beams while acting as an optical reference with spatial mode and noise filtering capabilities.

In this Letter, we present a CBC method utilizing a rigid-spacer bow-tie passive ring resonator as a single element to combine three high-power input beams, while simultaneously filtering the spatial mode, and power and frequency noise above the resonator's pole frequency of 1.2 MHz. Our CBC scheme further mitigates the effect of beam geometry fluctuations, which GWDs are highly sensitive to. A related experiment combined two low power laser beams inside a resonator for efficient second harmonic generation without usability of the combined beam in downstream experiments [13].

Figure 1 shows a schematic of the resonator with the three inputs, designated as beams 1–3. Each input beam is injected to co-propagate with the traveling wave mode of the ring resonator. The resonator is an adapted advanced LIGO pre-mode-cleaner (aLIGO PMC), as described in Refs. [3,14,15]. The same geometry is retained while retrofitted with mirrors near-optimized for the coherent combination of the three input beams.

A plane wave model was developed to optimize the reflectivity of the mirrors of the resonator. The plane wave model yields an output beam in terms of the field reflection and transmission coefficients, r_i and t_i, of input port i with input field E_i according to Fig. 1, as follows:

$$E_{\text{out}} = \frac{-t_{\text{out}}(t_1 E_1 + t_2 r_3 r_1 E_2 + t_3 r_1 E_3)}{1 - r_1 r_2 r_3 r_{\text{out}}}, \tag{1}$$

where t_{out} and r_{out} are the field coefficients for the output coupler. The summation of the input fields for 100% transmission is possible with different input mirror reflectivities and optimized phases. An exactly impedance matched cavity with a finesse of 124 requires input reflectivities of 99.58%, 98.64%, and 99.24%, for inputs 1, 2, and 3, respectively. While the differences in reflectivity are within manufacturing capabilities, the use of equal input mirror reflectivities would reduce the combining efficiency by approximately 0.5%. Figure 2 displays the results of the model with equal light power at each input and reflectivities of the input mirrors equalized and varied together.

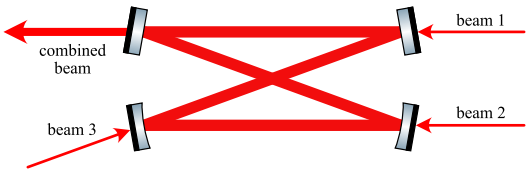

Fig. 1. Three-beam CBC with an optical ring resonator.

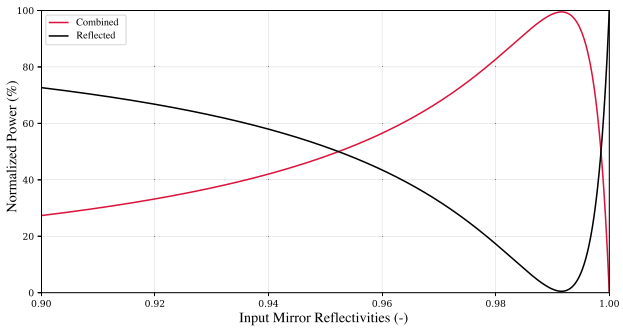

Fig. 2. Theoretical combining efficiency (red) and reflected power (black) versus input mirror reflectivity. Input mirror reflectivities and power injected at three input ports are identical. The output mirror reflectivity is 97.5%.

The output coupler is maintained with a reflectivity of 97.5%, used in the aLIGO PMC design. Total reflected power at the inputs reaches a minimum (0.5%) for an optimal combination of 99.5% with input and output reflectivities of 99.16% and 97.5%, respectively, maintaining a resonator finesse of 124. The model is easily generalized to an n-mirror resonator, yielding similar results and theoretically validating the prospects of scaling the number of inputs.

We demonstrate CBC for three inputs for which nearly optimal combination is expected for input and output reflectivities of 99.16% and 97.5%, respectively. We opted for identical input reflectivities, enabling a single coating run and an estimated worst-case reduction in combining efficiency of 0.7% due to manufacturing tolerances (+0.14%/−0.1%). The mirror substrates are super-polished with summed absorption and scattering losses below 10 p.p.m. with laser induced damage thresholds >10 kW/cm.

Figure 3 shows the layout of the bow-tie resonator CBC experiment. All three laser beams originate from an enhanced LIGO (eLIGO) front-end laser system [16], consisting of a non-planar ring-oscillator (NPRO) amplified by a Nd:YVO_4 amplifier. Extensive performance information for the system is available from its use in eLIGO, aLIGO, and GEO600 detectors [6,15,17]. The laser output is split by a half-wave plate and polarizing beam splitter into a low-power beam of 4 W and a high-power beam (beam 3) of 17 W. The low-power beam is amplified to 60 W of laser power by a neoVAN-4S-HP Nd:YVO_4 solid-state laser amplifier [4,5] and then split into beam 1 and beam 2 by a 50/50 beam splitter. The resulting three beams are attenuated to 10 W with variable attenuators (not shown). The polarization optics in the variable attenuators are also used to match the polarizations of the three beams before injection into the resonator. The combined beam leaves the resonator via the fourth port.

Three feedback control loops stabilize the frequency and phase of the beams for optimal coherent combination of the

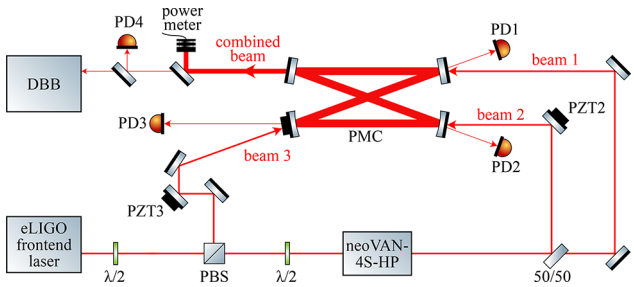

Fig. 3. Simplified optical layout. The three input beams originate from the same seed laser source (eLIGO front-end laser) that is split and partly amplified by a Nd:YVO_4 amplifier (neoVAN-4S-HP) and are injected into different ports of the resonator. Photodetectors (PD1–PD3) sense the reflected light at each input port for frequency and phase stabilization. Phase control signals are fed back to piezoelectrically controlled mirrors (PZT2 and PZT3). The combined beam leaves the fourth port of the resonator and is analyzed with photodetector PD4, a power meter, and an automatic beam diagnostic tool (DBB). (PBS, polarizing beam splitter; $\lambda/2$, half-wave retardation plate.)

circulating fields inside the resonator. An electro-optic modulator (not shown) inside the front-end generates phase modulation sidebands at 35.5 MHz for Pound–Drever–Hall (PDH) sensing schemes [18] utilizing photodetectors (PD1, PD2, and PD3) at the reflection of each input port. The PDH signal generated via PD1 is used to stabilize the laser frequency to the resonator with feedback from the NPROs frequency actuator. All three beams then have the same frequency, such that beams 2 and 3 are simultaneously kept on resonance. Without additional control, the phase relations between the three beams are random. The PDH signals generated via beams 2 and 3 are used to stabilize their respective phases with PZT-actuated mirrors for constructive interference of all three circulating fields inside the resonator, i.e., optimal coherent combination.

The spatial beam profile of each input beam is analyzed separately by measuring the power leaving port 4 as the laser frequency is scanned over a resonator free spectral range (FSR)

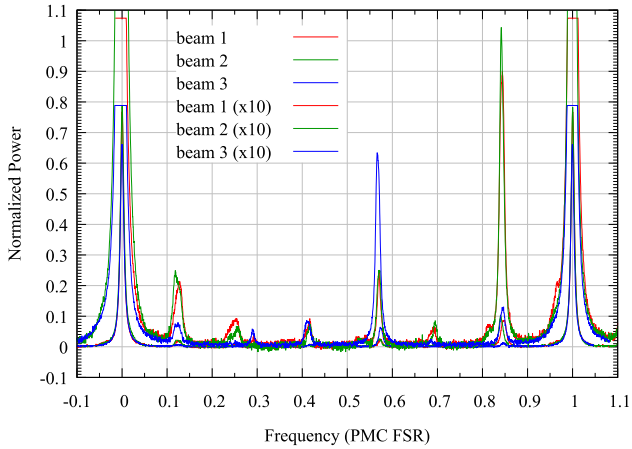

Fig. 4. Modescans of each input beam. For each measurement only one input beam was injected into the resonator, the length of which was scanned over one FSR. Whenever a mode of the input beam was resonant, the power on PD4 provides a measure of the relative contribution of this mode to the total power in the respective input beam.

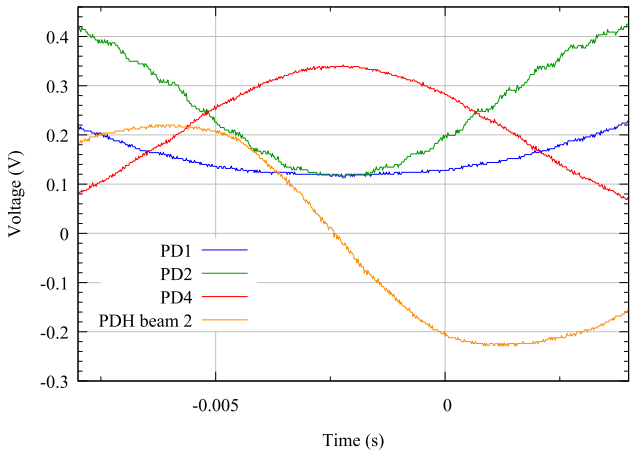

Fig. 5. Time series of the photodetector signals at ports 1, 2, and 4, alongside the PDH signals of beam 2 while the phase of beam 2 was ramped. The zero crossing of the PDH signal coincides with optimal combination of beams 1 and 2, maximizing power leaving the resonator (PD4) and minimizing the reflected power (PD1 and PD2). Beam 3 is blocked.

with the other two beams blocked. Figure 4 shows the normalized output power for the individual input beams. At 0 and 1 FSR, the fundamental cavity mode is resonant. For a better visibility of the small peaks that correspond to higher-order modes (HOMs) between 0.1 and 0.9 FSR we plotted a 10 times amplified version of the curves with thinner linestyle.

We calculated the HOM content of each input beam by summing the HOM peaks. The resulting HOM content was 23.4 %, 24.7 %, and 13.9 % for beams 1–3, respectively, significantly higher than is typical for this type of laser source. We attribute this to the aging of the pump diodes of the laser. Although generally unwanted, the larger HOM content allows us to demonstrate the mode-cleaning feature of our new CBC scheme. The power in HOMs is rejected by the resonator and hence the power in the spatially filtered combined beam is expected to be significantly below 30 W.

We locked the frequency of the front-end laser to the resonator using a servo loop with a unity gain frequency of 4.5 kHz with the PDH error signal from PD1. With beams 2 and 3 still blocked the transmitted beam was then characterized with an automatic beam characterization tool called the diagnostic breadboard (DBB) [19,20]. The HOM content of the output beam was calculated to be less than 0.22%. This indicates that the fundamental mode of the resonator is not distorted and close to a Hermite–Gauss HG_{00} mode, known to be the fundamental eigenmode of the DBB.

Figure 5 shows the time series of the power on PD1, PD2, and PD4, and the PDH error signal derived from PD2, with frequency stabilization via beam 1 engaged, beam 2 unblocked, and beam 3 blocked. The measurements were taken by scanning the phase of beam 2 using PZT 2 around the optimal combination point of beams 1 and 2. At the zero crossing of the PDH signal from PD2, the two beams are optimally combined inside the resonator such that the output power is maximized, as seen with PD4. Simultaneously, the power on PD1 and PD2 is minimized as the leakage field destructively interferes with the prompt reflection of input ports 1 and 2. Even for the optimal combination phase of beam 2, the power on PD1 and PD2 are not expected to reduce to zero due to the absence of beam 3. The circulating field is lower for this case with only two input beams, and hence, the interference of the leakage and promptly reflected field on PD1 and PD2 cannot be completely dark. Furthermore, there is a constant power on these PDs due to the HOM content of the input beams rejected by the resonator. Notably, the power on PD1–PD3 is close to the HOM power of each respective beam when all three beams are optimally combined. It is important to note that, while the parameters of beam 1 remained constant during this scan, the power on PD1 changed, which changes the open loop gain of the frequency stabilization control loop. Hence, sufficient gain margin and a robust design are required for stable operation of the feedback control loop while the phase of beam 2 is fluctuating. Similar behavior was observed when the phase of beam 3 is scanned while beam 2 is blocked.

Close to the CBC operation point the PDH error signals of beams 2 and 3 show a linear dependence on the phase of their respective input beams, having zero crossings coincident with maximal combined power to provide optimal error signals for the phase stabilization loops. As for the frequency stabilization control loop, a robust design of the phase stabilization loops is important, as the size of a particular PDH signal depends on the phases of the other beams. We successfully operated the phase control loops of beams 2 and 3 with measured unity gain frequencies of 187 Hz and 199 Hz, respectively. All control loops were robust and allowed for continuous operation of the CBC experiment for several hours, limited only by the dynamic range of the NPRO's frequency actuator.

With all input beams incident on the resonator and all control loops in operation, we measured a combined power of 21.2 W, which is 89 % of the estimated HG_{00} mode content of the three input beams (23.8 W). The input beams contained different HOM content, which results in an imbalance of optical power in the fundamental mode injected into each port of the resonator. Different power levels at the inputs effect impedance matching and result in a reduction of combination efficiency by several percent. Other losses are also expected in the system aside from HOM content and unbalanced light injection, including imperfect mode matching and additional losses within the resonator. Clipping was also observed in beam 3 along the input path to the resonator.

The spatial mode content of the combined beam was measured with the DBB. Figure 6 shows a modescan of the combined beam. The HOM content was calculated to be below 0.2 %, which is up to 100 times smaller than for the input beams. This impressively demonstrates the spatial mode filtering capability of our new CBC scheme. The peaks at 0.15 FSR and 0.65 FSR correlate to the resonances of the HG_{01} and HG_{10} modes associated with a misalignment of the beams with respect to the resonator's fundamental mode. Other peaks at 0.3 FSR and 0.6 FSR are caused by sub-optimal mode-matching, and the peak located at 0.5 FSR is due to a small polarization mismatch.

Figure 7 shows the relative power noise (RPN) of the combined beam with all control loops in operation. For comparison, the RPN of the beam leaving the output port is analyzed with only beam 1 injected and frequency stabilization engaged. The RPN of the combined beam is slightly increased with respect to the single beam measurement, which could be due to uncompensated phase noise in beam 2 or 3. Another possibility is greater beam pointing noise in beam 2 or 3 associated with slightly unstable mounts supporting the PZT mirror. This noise increase is less than one order of magnitude at all frequencies. It does not pose a problem for power stabilization systems typically used

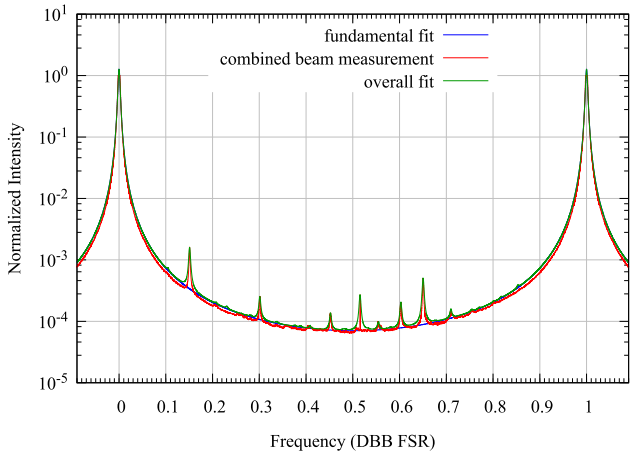

Fig. 6. Modescan of the combined beam leaving the resonator's output port, performed with the DBB. The HOM content of the combined beam is estimated to be <0.2%.

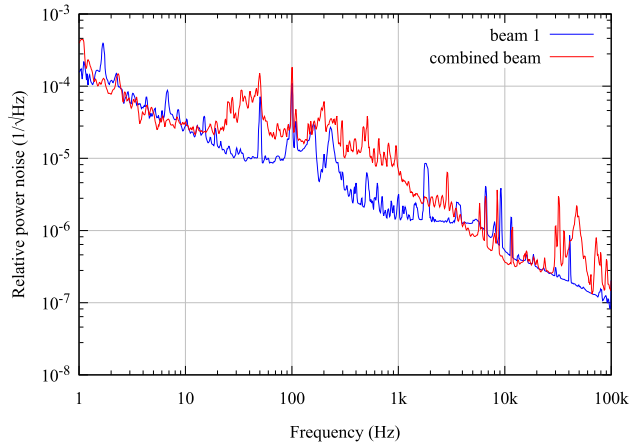

Fig. 7. Relative power noise measured with the DBB in transmission of the resonator.

in GWDs and other low-noise applications as it appears in a frequency band where down-stream power stabilization control loops can have large loop gain.

Elevated noise was also observed in a measurement of frequency noise with the DBB. This is likely due to uncompensated phase fluctuations in beams 2 and 3 that either directly influence frequency fluctuations in the circulating field or couple via the PDH error signals into the stabilization loops. Better shielding of the resonator against environmental disturbances and higher bandwidth phase control loops with increased low frequency gain could mitigate elevated frequency noise in the combined beam. As with RPN, the added noise will not limit fast frequency stabilization schemes typical to low noise experiments.

In conclusion, we have demonstrated a new scheme to coherently combine and spatially filter multiple laser beams by injecting them into an optical ring resonator with multiple input ports. The laser beams need to have identical frequencies that simultaneously matches a resonance frequency of the resonator. Once the phases of the injected light fields match, all beams interfere constructively inside the resonator and leave as a coherently combined light beam via the resonator's output port. The well-known PDH sensing scheme can be used to generate error signals for the frequency and phase stabilization loops that require robust design to cope with fluctuating loop gains during lock acquisition. We have combined three 10 W laser beams and demonstrated a HOM reduction of up to a factor of 100 with only marginal excess power and frequency noise in the combined beam. Our new filled-aperture CBC scheme can be used to generate high-power laser beams with the potential to serve as the pre-stabilized laser platform for next generation GWDs and is also highly applicable to industrial and scientific applications requiring ultra-stable, single-frequency, diffraction-limited laser sources.

Funding. Deutsche Forschungsgemeinschaft(DFG, German Research Foundation) under Germany's Excellence Strategy – EXC-2123 QuantumFrontiers – 390837967; National Science Foundation (PHY-1806634); Australian Research Council (CE170100004).

Disclosures. The authors declare no conflicts of interest.

Data availability. Data underlying the results presented in this paper are not publicly available at this time but may be obtained from the authors upon reasonable request.

REFERENCES

1. ET Steering Committee, "ET design report update 2020," Tech. Rep. (2020).
2. K. Ackley, V. B. Adya, and P. Agrawal, *et al.*, Publ. Astron. Soc. Aust. **37**, e047 (2020).
3. P. Kwee, C. Bogan, K. Danzmann, M. Frede, H. Kim, P. King, J. Pöld, O. Puncken, R. L. Savage, F. Seifert, P. Wessels, L. Winkelmann, and B. Willke, Opt. Express **20**, 10617 (2012).
4. F. Thies, N. Bode, P. Oppermann, M. Frede, B. Schulz, and B. Willke, Opt. Lett. **44**, 719 (2019).
5. N. Bode, F. Meylahn, and B. Willke, Opt. Express **28**, 29469 (2020).
6. N. Bode, J. Briggs, X. Chen, M. Frede, P. Fritschel, M. Fyffe, E. Gustafson, M. Heintze, P. King, J. Liu, J. Oberling, R. L. Savage, A. Spencer, and B. Willke, Galaxies **8**, 84 (2020).
7. J. W. Dawson, M. J. Messerly, R. J. Beach, M. Y. Shverdin, E. A. Stappaerts, A. K. Sridharan, P. H. Pax, J. E. Heebner, C. W. Siders, and C. P. J. Barty, Opt. Express **16**, 13240 (2008).
8. G. A. Kerr and J. Hough, Appl. Phys. B **49**, 491 (1989).
9. H. Tünnermann, J. H. Pöld, J. Neumann, D. Kracht, B. Willke, and P. Wessels, Opt. Express **19**, 19600 (2011).
10. L.-W. Wei, F. Cleva, and C. N. Man, Opt. Lett. **41**, 5817 (2016).
11. N. Bode, "Characterization, stabilization and coherent combination of high power laser beams for gravitational wave detectors," Ph.D. thesis, Gottfried Wilhelm Leibniz Universität Hannover (Germany) (2023).
12. F. Wellmann, N. Bode, P. Wessels, L. Overmeyer, J. Neumann, B. Willke, and D. Kracht, Opt. Express **29**, 10140 (2021).
13. G. Ferrari, J. Catani, L. Fallani, G. Giusfredi, G. Schettino, F. Schäfer, and P. C. Pastor, Opt. Lett. **35**, 3105 (2010).
14. J. H. Pöld, "Aligo bow-tie pre-modecleaner document," Tech. Rep. LIGO-T0900616-v3 (2012).
15. J. Pöld, "Design, implementation and characterization of the advanced ligo 200wlaser system," Ph.D. thesis, Gottfried Wilhelm Leibniz Universität Hannover (Germany) (2014).
16. M. Frede, B. Schulz, R. Wilhelm, P. Kwee, F. Seifert, B. Willke, and D. Kracht, Opt. Express **15**, 459 (2007).
17. K. L. Dooley and LIGO Scientific Collaboration, J. Phys.: Conf. Ser. **610**, 012015 (2015).
18. E. D. Black, Am. J. Phys. **69**, 79 (2001).
19. P. Kwee and B. Willke, Appl. Opt. **47**, 6022 (2008).
20. P. Kwee, "Laser characterization and stabilization for precision interferometry," Ph.D. thesis, Gottfried Wilhelm Leibniz Universität Hannover (Germany) (2010).